The Density and Refractive Index of Adsorbing Protein Layers

Janos Vörös

BioInterface Group, Laboratory for Surface Science and Technology, ETH Zurich, Schlieren, Switzerland

ABSTRACT   The structure of the adsorbing layers of native and denatured proteins (fibrinogen, γ-immunoglobulin, albumin, and lysozyme) was studied on hydrophilic TiO_2 and hydrophobic Teflon-AF surfaces using the quartz crystal microbalance with dissipation and optical waveguide lightmode spectroscopy techniques. The density and the refractive index of the adsorbing protein layers could be determined from the complementary information provided by the two in situ instruments. The observed density and refractive index changes during the protein-adsorption process indicated the presence of conformational changes (e.g., partial unfolding) in general, especially upon contact with the hydrophobic surface. The structure of the formed layers was found to depend on the size of the proteins and on the experimental conditions. On the TiO_2 surface smaller proteins formed a denser layer than larger ones and the layer of unfolded proteins was less dense than that adsorbed from the native conformation. The hydrophobic surface induced denaturation and resulted in the formation of thin compact protein films of albumin and lysozyme. A linear correlation was found between the quartz crystal microbalance measured dissipation factor and the total water content of the layer, suggesting the existence of a dissipative process that is related to the solvent molecules present inside the adsorbed protein layer. Our measurements indicated that water and solvent molecules not only influence the 3D structure of proteins in solution but also play a crucial role in their adsorption onto surfaces.

INTRODUCTION

The adsorption of proteins at solid-liquid interface is an extensively studied research field because of its importance and relevance in biosensor and biomaterial applications (Cooper, 2002; Kasemo, 2002; Mathieu, 2001). The adsorption process involves the transport of proteins from the solution to the interface, their binding to the surface usually via hydrophobic and electrostatic interactions, and their relaxation on the surface via conformational changes (Malmsten, 2000; Norde, 2000; Ramsden, 1997). Water molecules, solvated ions, and other small molecules in the vicinity of the surface and the proteins play an important role in this process by mediating both the hydrophobic and the electrostatic interactions and by determining the secondary and tertiary structure of the adsorbing molecules (Tsai et al., 2002; Vogler, 1998). An adsorbed layer of proteins contains more ions and water than proteins, and the presence of a chaotropic agent not only destabilizes the structure of the protein but also influences its adsorption properties (Henderson, 2002).

Several label-free, in situ detection techniques were developed to monitor the adsorption of proteins: surface plasmon resonance (Baird and Myszka, 2001; Rich and Myszka, 2002), ellipsometry (Arwin, 2000), optical waveguide lightmode spectroscopy (OWLS) (Voros et al., 2002), reflectometry (Schaaf et al., 1987a,b), and the resonant mirror (Skladal and Horacek, 1999) techniques measure the changes in the refractive index at the interface; quartz crystal microbalance (QCM) (Glasmastar et al., 2002; O'Sullivan and Guilbault, 1999), and surface acoustic wave devices (Welsch et al., 1996) measure the frequency changes of an oscillating quartz crystal upon adsorption of a protein layer. Whereas the refractive index change is usually directly related to the amount of protein molecules present in the adsorbed layer, the frequency changes of the QCM and surface acoustic wave devices are connected to the total mass (including the water and ions) coupled onto the surface. Recently the combination of these techniques is emerging to fulfill the need for getting more reliable and complementary data on different complicated surface processes (Bailey et al., 2002; Hook et al., 2001; Laschitsch et al., 2000; Otzen et al., 2003; Picart et al., 2001; Stalgren et al., 2002; Vikinge et al., 2000). In a recent study, we showed that the combination of optical techniques with quartz crystal microbalance with dissipation (QCM-D) is particularly useful when studying the adsorption of proteins to surfaces (Hook et al., 2002).

In this work we further extend the previously published investigations and show how the complementary information provided by the OWLS and the QCM-D factor monitoring technique can be used to study the structure of the adsorbed protein layers. Four proteins (fibrinogen, γ-immunoglobulin, albumin, and lysozyme) with different sizes and shapes were adsorbed onto a hydrophilic TiO_2 and onto a hydrophobic Teflon-AF surface whereby the changes in density and refractive index of the layers were determined as a function of adsorption time.

MATERIALS AND METHODS

Coating of the sensor chips

Commercially available planar optical waveguides (2400 μV, Micro-Vacuum, Budapest, Hungary) and QCM sensor crystals (Q-Sense AB,

---

Goteborg, Sweden) were used during the experiments. The sensitive surface of the QCM sensors is the gold electrode, while the waveguides contain ~75% SiO_2 and 25% TiO_2 on their surface (Kurrat et al., 1997; Yoldas, 1982).

A 12-nm TiO_2 layer was magnetron-sputtered onto the QCM chips and the waveguides to ensure that the protein adsorption measurements were not influenced by the properties of their original surfaces. This 12-nm TiO_2 layer was found to be sufficiently thick to hinder the properties of the underlying substrate materials but also thin enough not to alter the sensitivity of the sensors (Kurrat et al., 1997). The TiO_2-coated waveguides and QCM chips were cleaned in oxygen plasma (Harrick, Ossining, NY) for 1 min prior to the measurements.

Spin-coating of thin polymer layers, such as phosphorylcholine-containing polyurethanes and ultrahigh-molecular-weight polyethylene, onto the optical waveguides has been previously demonstrated in our laboratory (Ruiz et al., 1999; Widmer et al., 2001). In this study Teflon-AF (Dupont, Wilmington, DE) was spin-coated onto the gold electrodes of the QCM chip and onto the waveguides using a home-built instrument at 1800 rpm to achieve a chemically stable, hydrophobic surface. The thickness of the coating could be easily varied by diluting the Teflon-AF solution with FC-43 solvent (Dupont). The Teflon-AF concentration used in this study was 10%.

The waveguides and the QCM chips were cleaned in oxygen plasma for 1 min prior to the coating. Thirty minutes of annealing at 150°C was required to remove physisorbed water and 20 min of hexamethyl-disilazane (Sigma, Fort Collins, CO) vapor silanization of the optical waveguides was necessary before the spin-coating to enhance the adhesion of the Teflon layer.

The coated QCM chips and waveguides were annealed at 150°C in air for 1 h and used for the measurements immediately.

The chemical integrity of the coated sensor chips was confirmed by x-ray photoelectron spectroscopy (Fig. 1) and contact angle measurements (Krüss, Hamburg, Germany). The topography was characterized using atomic force microscopy, and the coating process was also monitored by QCM-D and OWLS (results not shown). Contact angles of 121° ± 1° and <6° were measured on the Teflon-AF and TiO_2 coated surfaces, respectively, for both underlying substrates.

OWLS

The OWLS technique uses an optical grating for the incoupling of a He-Ne laser into a planar waveguide. It allows for the precise measurement of the
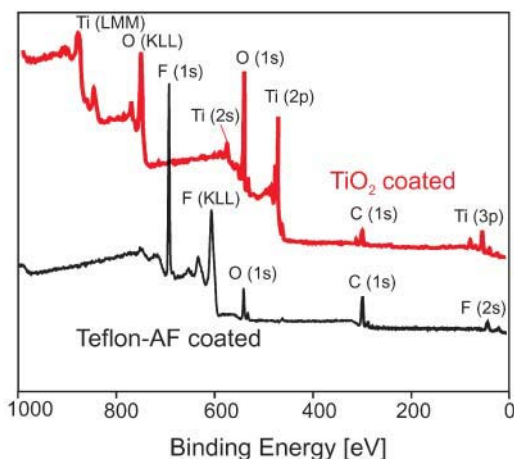

FIGURE 1   X-ray photoelectron spectroscopy survey spectra of the TiO_2 and Teflon-AF coated sensor surfaces. Besides the inevitable hydrocarbon contamination, only Ti and O related peaks are present in the spectra of the TiO_2 coated quartz crystal and only F- and O-related peaks are present in the spectra of the Teflon AF coated waveguide, indicating the presence of a complete coating in both cases.

change in the phase-shifts of the transverse electric and transverse magnetic polarization modes of the laser upon adsorption of macromolecules. The optical thickness and the refractive index of thin and homogeneous adsorbed layers can be determined from the phase shifts as described in Tiefenthaler and Lukosz (1989). Since the refractive index is a linear function of the concentration over a wide range of concentrations, the absolute amount of the adsorbed molecules can be calculated using de Feijter's formula (de Feijter et al., 1978):

$$M = d_A \frac{n_A - n_C}{dn/dc}, \qquad (1)$$

where d_A is the thickness of the adsorbed layer and dn/dc is the refractive index increment of the molecules, which can be measured using a refractometer. The surface adsorbed mass densities determined from Eq. 1 depend only on the difference in the refractive index of the adsorbed molecules (n_A) and the cover medium (n_C); thus the coupled solvent molecules will not contribute to the mass.

The OWLS technique is highly sensitive (i.e., ~1 ng/cm^2) and allows for the direct online monitoring of macromolecular adsorption.

QCM-D

QCM-D is a technique for monitoring the mass of adsorbed molecules via changes in the resonant frequency, Δf, while also getting information about the viscoelasticity of the layer by measuring the dissipation factor, D. In contrast to the OWLS, which is not sensitive to water associated with adsorbed proteins; the f-shift of the QCM-D is due to the change in the total coupled mass, including the water coupled to the layer.

The Sauerbrey equation establishes the relationship between the measured frequency change (Δf) and the adsorbed mass per unit area (M) for rigid adsorbed layers:

$$M = -\frac{C}{n}\Delta f, \qquad (2)$$

where C (=17.7 ng cm^{-2} Hz^{-1} for f = 5 MHz crystals) is the mass sensitivity constant and n (=1,3,...) is the overtone number. For viscoelastic layers measured in liquid environment this equation underestimates the adsorbed mass (Hook et al., 2001). However, for the thin protein layers in this study this difference was always <10% as estimated from the frequency shifts of the different overtones using the Voigt-Kelvin model (Voinova et al., 2002).

Experimental

Proteins with significant differences in their sizes ranging from 14.3 kD to 340 kD were chosen for the experiments. The adsorption of chicken egg white lysozyme (Lys), human serum albumin (HSA), human fibrinogen (Fb) (Sigma), and human γ-immunoglobulin (IgG) (Roche, Basel, Switzerland) was measured on TiO_2 in HEPES buffer (10 mM N'(2-hydroxyethyl) piperazine-N-ethanesulphonic acid (Sigma), pH 7.4) using two different concentrations, 40 and 80 μg/mL. The adsorption of the same proteins at a concentration of 40 μg/mL was also tested on the Teflon-AF coated hydrophobic surfaces. The adsorption of the denatured forms of the same proteins was also measured on TiO_2 in the presence of 6 M urea (Sigma), a chaotropic agent.

The measurements were made at 25°C according to the following protocol. After a stable baseline was achieved the protein solution was added into the measuring chambers of the OWLS (BIOS-1, ASI AG, Zurich, Switzerland) and the QCM-D (Q-Sense) and the adsorption process was monitored until saturation, followed by a final rinsing step. Static conditions were chosen for the measurements to avoid complications due to the

different flow-cell geometries of the two instruments (axial flow-cell in the QCM-D versus laminar flow-cell in the OWLS). The liquid exchange was instantaneous using a syringe injection.

Usually three, but in the case of very good reproducibility (<1% deviation between curves) a minimum of two, adsorption curves were recorded with each technique for all proteins and experimental conditions. The difference between the measurements was always <10%. The OWLS-derived mass was determined according to Eq. 1 using 0.182 g/cm^3 for the dn/dc of the proteins. The QCM-derived mass was determined from Eq. 2 using the frequency shift of the seventh overtone of the quartz crystal.

RESULTS

Protein adsorption curves

The adsorption curves of the different proteins at different experimental conditions are summarized in Fig. 2. The QCM-D measures higher adsorbed mass values for all the proteins under all experimental conditions.

If we look at the adsorption curves of Fb at different experimental conditions (see Fig. 2 a) on TiO$_2$ we find that after 30 min more Fb adsorbs from a higher concentration, but the adsorbed mass is less in the presence of 6 M urea. However, the two measurement techniques provide remarkably different results for the adsorbed amounts on the AF-Teflon surfaces: the QCM-D measures ~70% higher amounts, whereas the OWLS shows 20% lower adsorbed mass compared to the adsorption onto the TiO$_2$ surface using identical solution conditions (40 μg/mL Fb in HEPES).

The IgG adsorption on TiO$_2$ is qualitatively similar to Fb (see Fig. 2 b). After 30 min adsorption time the highest mass is observed for the high concentration, lower values are obtained for the lower concentration, and the denatured protein shows the least adsorption. The adsorption onto AF-Teflon is again different: the QCM-D measures only ~10% less adsorbed IgG on AF-Teflon than on TiO$_2$, whereas the OWLS shows a 60% decrease.

If we only look at the OWLS curves, the adsorption of HSA onto TiO$_2$ seems to be similar to IgG and Fb (see Fig. 2 c): after 30 min the highest adsorption is observed at the higher concentration, lower at the lower concentration, and the lowest value for the denatured proteins. However, if we look at the QCM curves this order is changed. Although the adsorbed mass of the higher concentration is still higher than the low concentration, the denatured proteins show the highest adsorption. The lowest adsorbed amounts are measured on the hydrophobic AF-Teflon with both methods.

The Lys adsorption curves show an interesting coincidence for the QCM-D (Fig. 2 d): only a minor difference is seen between the adsorption of the denatured and the native proteins. But the OWLS measurements again show the lower adsorption values in the presence of 6 M urea. On the AF-Teflon both techniques measure much less adsorbed mass compared to the results on TiO$_2$.

Density changes of the adsorbed protein layer

The difference between the OWLS-derived ''dry'' mass value and the QCM-D-derived ''wet'' mass can be attributed to the solvent molecules present in the adsorbed protein layer. The density of this layer can also be estimated using (Hook et al., 2001):

$$\rho_{layer} = \frac{m_{QCM}}{\frac{m_{OWLS}}{\rho_{protein}} + \frac{m_{solvent}}{\rho_{solvent}}}, \qquad (3)$$

where $m_{solvent}$ denotes the total mass per unit area of solvent molecules present inside the protein layer calculated from the formula $m_{solvent} = m_{QCM} - m_{OWLS}$. The density of the HEPES was 1.000 g/cm^3 without and 1.058 g/cm^3 with the 6 M urea as measured with a pycnometer at 25°C, while the literature value of $\rho_{protein} = 1.33$ g/cm^3 was used for the proteins (Hook et al., 2002; Tsai et al., 1999). The evolution of the changes in the density of the adsorbed protein layer can be followed by calculating ρ_{layer} at each time point of the measurements using Eq. 3. The obtained density curves provide a rich insight into the conformational changes occurring during the adsorption process.

On the TiO$_2$ surface the density increment of Fb after going through a small maximum quickly reaches a stable value at ~0.08 g/cm^3 when adsorbed from the HEPES buffer (see Fig. 3 a). Using higher concentration speeds up this process and a slightly denser, thicker protein layer is formed. In the presence of 6 M urea, the layer of denatured proteins has a significantly lower final density increment (0.05 g/cm^3) and longer time is needed to reach saturation. The lowest adsorbed protein layer density increment (0.04 g/cm^3) was found on the AF-Teflon.

The density increment of the adsorbed IgG layer is higher than for Fb in the HEPES buffer (0.1 g/cm^3), but it is lower when the layer is made of denatured proteins (see Fig. 3 b). Using a higher concentration again speeds up the formation of the packed layer when adsorbing from the HEPES buffer. The curve goes through a small maximum similarly to the Fb case if 80 μg/mL IgG concentration is used but no maximum is observed for the lower concentration. The adsorbed IgG is less dense on the AF-Teflon than on the TiO$_2$ similarly to Fb, but the saturation density increment on the AF-Teflon is higher than the density increment of the adsorbed denatured IgG layer on the TiO$_2$.

The HSA layer also has a very low density increment in the presence of the chaotropic agent, similarly to the IgG (0.03 g/cm^3) (see Fig. 3 c). On the hydrophobic surface the density increment of the adsorbed HSA layer first goes through a maximum after 2 min then decreases during the adsorption process reaching a steady state at ~0.12 g/cm^3, which is close to the value measured on the hydrophilic surface. HSA forms a slightly less dense layer when adsorbing onto TiO$_2$ from a more concentrated solution.
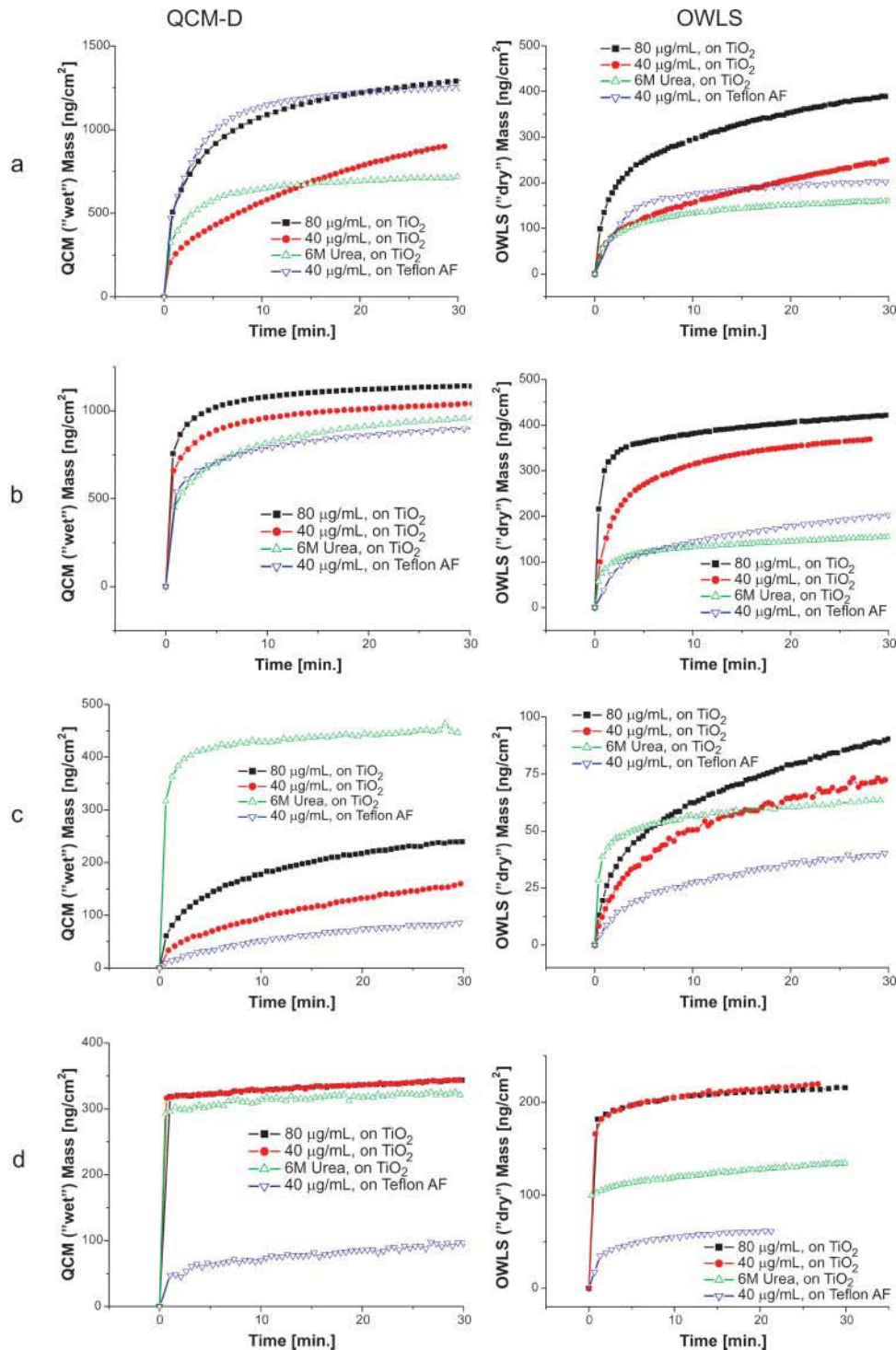
FIGURE 2 The evolution of the adsorbed mass of (*a*) Fb, (*b*) IgG, (*c*) HSA, and (*d*) Lys layers as obtained from the QCM-D and OWLS techniques. The adsorption of proteins was tested from HEPES (with and without 6 M urea) using 40- and 80-μg/mL concentrations on the hydrophilic TiO_2 and on the hydrophobic Teflon-AF.

The adsorbed Lys layer has the highest density of all the proteins studied. The layer density is also lower in the presence of 6 M urea similarly to the other proteins (see Fig. 3 *d*). The curves saturate smoothly on the TiO_2, whereas on the AF-Teflon a very high (0.24 g/cm^3) density increment is reached almost instantaneously.

Dissipation factor

A linear correlation was found between the dissipation factor and the total amount of water (m_{water}) present in the adsorbed protein layer for all proteins and experimental conditions (see Fig. 4). The slope of the dissipation factor versus total
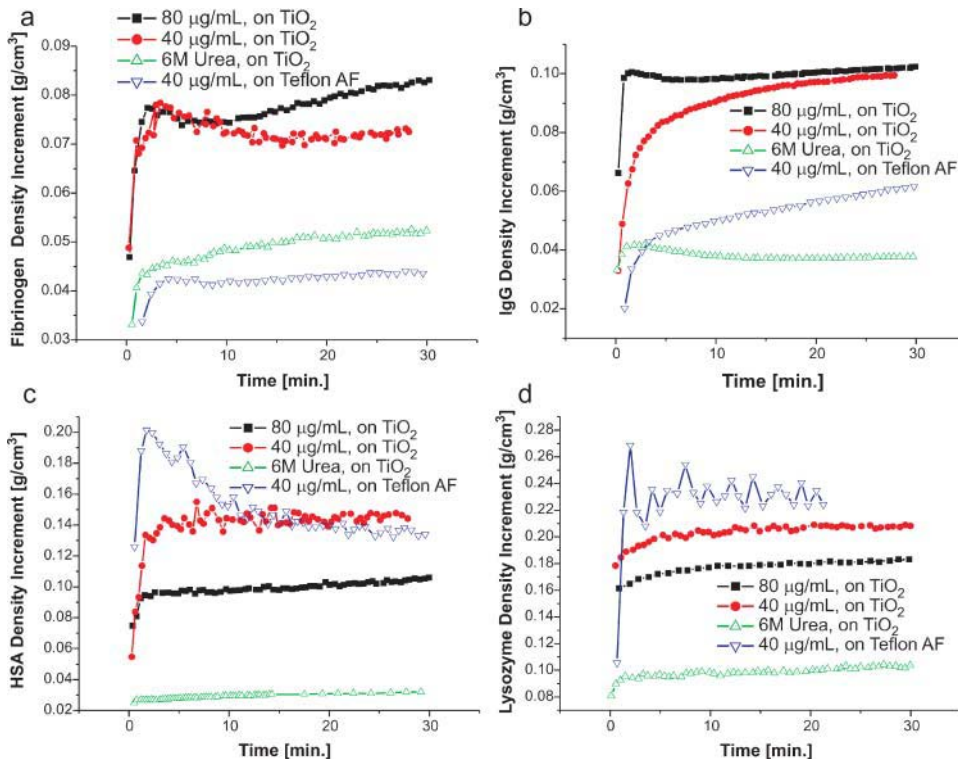
FIGURE 3 Changes in the density increment of the adsorbed (*a*) Fb, (*b*) IgG, (*c*) HSA, and (*d*) Lys layers during the adsorption process. The density of the layers was calculated using the QCM-D-derived ''wet'' and the OWLS-derived ''dry'' masses according to Eq. 3.

water content curves generally depended on two of the experimental conditions, the surface and the solvent, except in the case of HSA, where a uniform slope of 4.23 ± 0.01 $[\mu g/cm^2]^{-1}$ was found (see Fig. 4 *c*).

In the case of Fb small deviations from the linearity were observed when adsorbing onto the TiO_2 from the HEPES buffer (see Fig. 4 *a*). However, the initial slopes of these curves were similar to the value found for HSA. Good linearity but a higher slope was obtained for the denatured Fb. A lower slope was measured if adsorbing onto AF-Teflon.

In the case of IgG on the TiO_2 surface the slopes of the dissipation factor water content curves are slightly lower than for HSA both if adsorbing from the HEPES buffer and if the 6 M urea is used (see Fig. 4 *b*). On the AF-Teflon the slope of the curve is very similar to that of the Fb.

For Lys again the higher water content corresponds to more dissipative losses although due to the low dissipation factor values and the fast adsorption kinetics only the experimental noise is visible on the curves (see Fig. 4 *d*).

Refractive index of adsorbed protein layers

Both the density and the refractive index of a protein solution are linear functions of the protein concentration. Thus the measurement of the density of the adsorbed protein layer allows for the determination of the refractive index of the layer using the following equation:

$$n_{\text{layer}} = n_{\text{solvent}} + \frac{\rho_{\text{layer}} - \rho_{\text{solvent}}}{1 - \frac{\rho_{\text{solvent}}}{\rho_{\text{protein}}}} \frac{dn}{dc}. \qquad (4)$$

The values 1.33156 and 1.38483 were measured for the refractive index of HEPES without and with 6 M urea, respectively, at 25°C using a refractometer from Zeiss (Jena, Germany). Although the refractive index increment of protein solutions has been reported to depend on the buffer conditions, we have found no difference from the generally accepted literature value of $dn/d = 0.182$ g/cm³ within the 20% uncertainty of our measurements (Ball and Ramsden, 1998; de Feijter et al., 1978).

The density and the refractive index of the protein layers after 30 min of adsorption show a clear dependence on the size of the molecules. Whereas the density of the adsorbed Lys layer is ~1.18 g/cm³, which corresponds to a refractive index for the layer of 1.48, proteins with larger molecular weight form a less dense layer in the HEPES buffer (Fig. 5). In the presence of 6 M urea the formed layers have similar densities (corresponding to a lower density increment because of the denser solvent) and a slight increasing tendency is observed toward the higher molecular weight proteins with the exception of Lys.

DISCUSSION

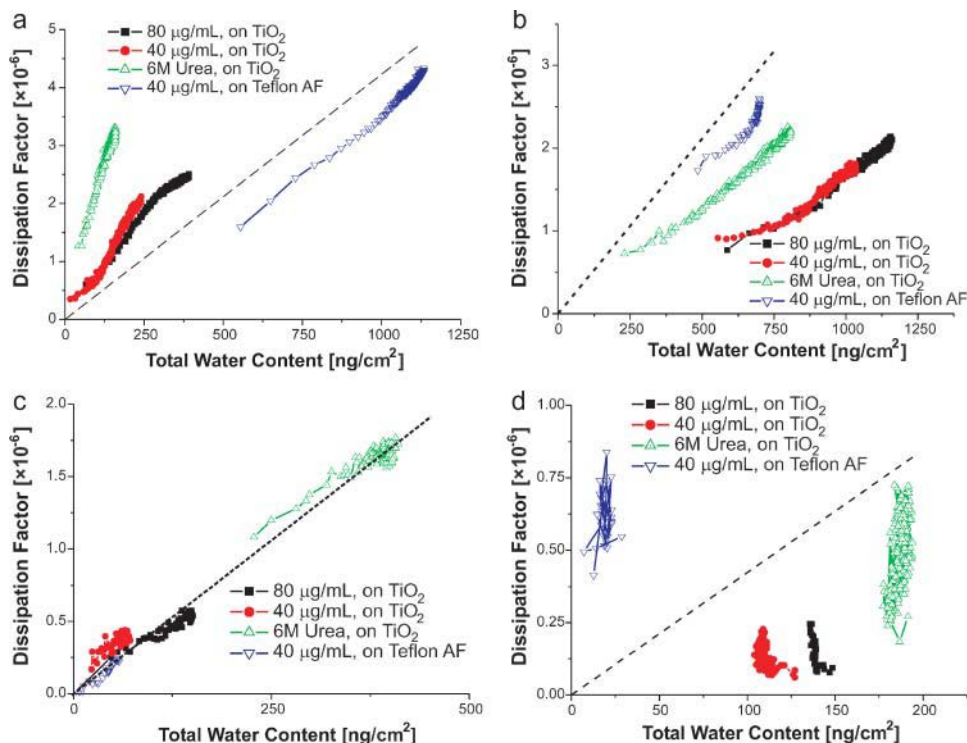The adsorbed mass measured by the QCM-D technique was derived form the frequency shift using the Sauerbrey

FIGURE 4 Correlation between the total water content of the protein layer and the QCM-D dissipation factor for (a) Fb, (b) IgG, (c) HSA, and (d) Lys. The lines indicate the uniform linear correlation that was found in the case of HSA for all experimental conditions.

equation. This equation is only strictly valid for rigid, nonporous, homogeneous adlayers and it has been shown that taking the viscoelastic properties of the adsorbed layer into account adds a correction to the Sauerbrey mass. This correction depends on the dissipation factor and the layer thickness. For thin layers it is always positive and in our case it is always below 10% (Reimhult et al., 2003; Voinova et al., 2002).

The OWLS technique measures the refractive index and the thickness of the adsorbed layer assuming a homogeneous, thin film (<50 nm) on the surface (Lukosz, 1991). The thickness assumption is fulfilled because the adsorbed layer thickness was always smaller than 12 nm for all of the experiments. However, during the adsorption of the molecules the homogeneity condition does not hold because the surface has both covered and uncovered regions on the nanometer scale. Since the OWLS technique averages over the laser-illuminated area (1 mm^2) the determined thickness is not the true height of the adsorbed molecules but the average height times the surface coverage. The calculated refractive index is the refractive index of the ''dry'' molecules because the calculation is based on the refractive index difference between the analyte and the solvent (see Fig. 6). These effects were only studied on the micron scale (Horvath et al., 2001), but they cancel out when determining the adsorbed mass using de Feijter's formula, where the contribution of the noncovered regions is zero (see Eq. 1) (Mann, 2001).

Based on the discussion above and on previous results, it can be accepted that the difference between the QCM-D and

OWLS-derived mass is due to the solvent molecules coupled to the adsorbed protein layer (see Fig. 6). This has also been published earlier by Hook et al., and it explains why the QCM-D derived mass is higher for all of the proteins and all experimental conditions (Hook et al., 2001, 2002; Voinova et al., 2002) (see Fig. 2).

It is widely reported that the adsorbed amount of proteins is higher when adsorbing from higher concentrations, as in the case of our experiments (see Fig. 2), although no detailed theoretical explanation of this phenomenon has been given to date (Norde, 2000).

The amount of denatured proteins adsorbed onto hydrophilic surfaces was found to be less than the adsorption amount of native proteins and only slightly higher than the amount of native proteins adsorbed onto the hydrophobic Teflon-AF indicated by the OWLS results in Fig. 2. These are reasonable results since the denatured proteins have a random coil structure that can occupy a larger area on the surface than their more compact native conformation (Kull et al., 1997). The very different QCM-D results obtained for the denatured proteins can be explained by the different solvent content of the studied protein layers.

Although most researchers agree that the solvent molecules contribute to the QCM-D signal there are still several open questions where there is no consensus in the literature:

Where is the solvent which is sensed by the QCM-D? Is it only the solvent molecules inside and at the surface of the proteins that contribute to the QCM-D signal, or is all the solvent that is present in the adsorbed layer also measured?
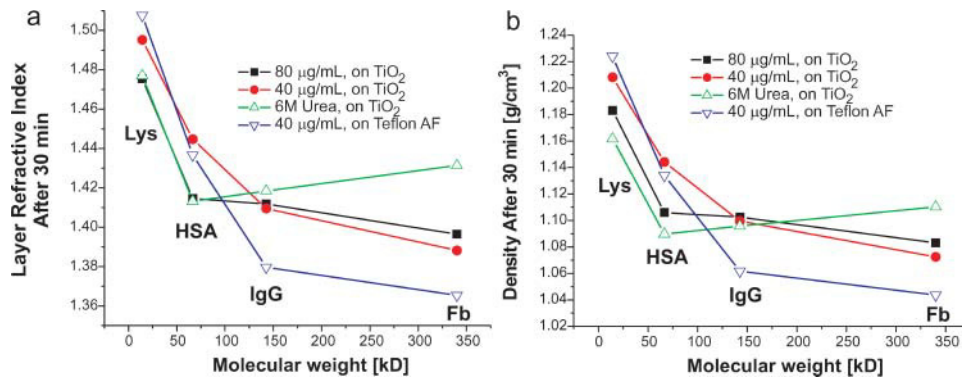
FIGURE 5 The refractive index (*a*) and the density (*b*) of the saturated protein layers after 30 min of adsorption are plotted as a function of the molecular weight. Smaller proteins can form denser layers than the larger ones.

The partial specific volume of proteins is smaller than 0.75 mL/g which corresponds to densities close to or larger than 1.33 g/cm^3 (Arosio et al., 2002; Tsai et al., 1999). The difference between our QCM-D and OWLS measurements is so large that the highest calculated protein layer density is still much lower than this value, indicating that the QCM-D technique also measures the solvent molecules that are present between the adsorbed protein molecules inside the layer (see Figs. 3 and 6). This is also confirmed by the excellent agreement between our calculated density data and neutron reflectivity measurements. Lu et al. (1998) have shown that a thin ($\sim$1 nm) but dense Lys layer is formed on a hydrophobic surface where the volume fraction of Lys is 0.85, corresponding to a layer density of 1.28 g/cm^3, whereas a much thicker ($\sim$6 nm) but less dense Lys layer is formed on a hydrophilic surface (Lu et al., 1998).

What can we learn from the time dependence of the density changes in an adsorbing protein layer? Most of the density curves in Fig. 3 show that the density of a protein layer is continuously increasing until reaching a value which

is characteristic of the protein, the surface, and the experimental conditions. This corresponds to the simple picture of the random sequential adsorption model: the adsorbing proteins sequentially occupy the available surface (Ramsden, 1993; Talbot et al., 2000). (See adsorption of HSA on TiO$_2$ for a typical example in Fig. 3 *c*.) Other curves show more complex behavior. The formation of a thin and dense unfolded HSA layer on the hydrophobic surface is followed by further adsorption of HSA molecules which have insufficient free surface left for a complete denaturation. These molecules are often considered as a ''second layer'' since their density is similar to the native proteins adsorbing to the hydrophilic surface as can be seen in Fig. 3 *c* (Lu et al., 1998).

The found linear correlation between the dissipation factor and the total water content of the layer suggest the existence of a dissipative process that is related to the solvent molecules present inside the adsorbed protein layer. The QCM-D technique probes processes with relaxation times in the 10^{-7}-s range because the frequency of the quartz crystal oscillations is in the 10^7-Hz range. If the time which the solvent molecules spend immobilized inside the adsorbed protein layer is comparable to the characteristic time of the oscillations then the energy taken away by these molecules can be responsible for most of the dissipative losses of the quartz crystal.

In the literature the refractive index of adsorbed protein layers is usually preset and its assumed value varies between 1.35 and 1.6 in ellipsometry and surface plasmon resonance calculations (Benesch et al., 2002; Jung et al., 1998). This assumption is inherently equivalent to assuming a certain density for the adsorbing protein layer according to Eq. 4 and as such it can easily result in the incorrect interpretation of the layer-forming process. Although the optical layer thickness calculated this way is misleading and has no obvious connection to the real dimensions of the molecular layer, the surface adsorbed mass densities calculated from this layer thickness are still correct.

Our results have shown that contrary to the usual assumptions, the density of the adsorbing protein layer is not constant during the adsorption process, and that the
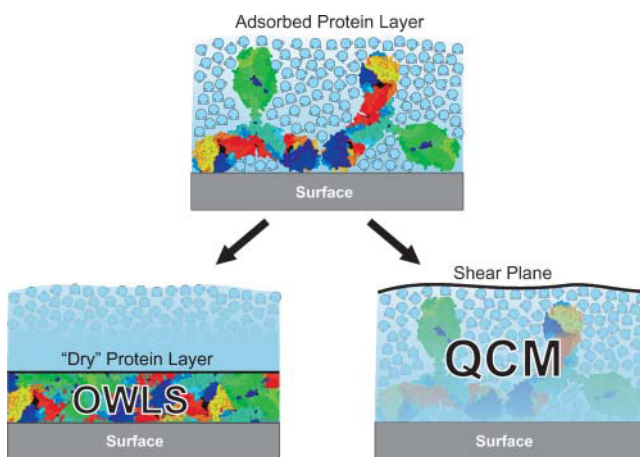

FIGURE 6 Illustration of the difference between the measuring techniques: OWLS is only sensitive to changes in the refractive index; thus it measures the ''dry'' mass of the adsorbed molecules, whereas the QCM-D oscillations drag every molecule below the shear-plane and as such measure the ''wet'' mass of the adsorbed layers.

density of the saturated protein layers depends on the size of the molecules and also on the experimental conditions (Fig. 3). Smaller proteins (i.e., Lys) form a more compact layer with a higher density and refractive index than large proteins (i.e., Fb) (Fig. 5 *b*). The calculated refractive index values fall between the refractive index of the solvent and the refractive index of dried protein layers (1.53), which is in good agreement with our expectations (Fig. 5 *a*) (Benesch et al., 2002; Schaaf et al., 1987a).

CONCLUSIONS

The density changes in the adsorbing layers of four proteins (Fb, IgG, HSA, and Lys) were measured using two complementary in situ biosensor techniques, OWLS and QCM-D. The proteins were adsorbed onto hydrophilic TiO_2 and hydrophobic AF-Teflon surfaces using two different concentrations from two different buffers (HEPES with and without 6 M urea) to test the effect of the experimental conditions on the density of the adsorbed layer.

The density of the protein layer was found to change during the adsorption process and the density at saturation depended on the size of the proteins: smaller proteins formed a denser layer than larger ones. The layers had a lower density on the hydrophilic TiO_2 if unfolded proteins were adsorbed. The hydrophobic surface-induced denaturation resulted in a formation of thin compact protein films with higher density increments for HSA and Lys.

For the refractive indices of the adsorbed layers realistic values between 1.36 and 1.55 were obtained depending on the size of the proteins and the experimental conditions. The dissipation factor measured by the QCM-D correlated very well with the amount of solvent present in the adsorbed protein layer, suggesting that the solvent molecules are mainly responsible for the dissipative losses in thin protein films.

It was clearly shown that the density and refractive index of the adsorbed protein layer are changing during the adsorption process and largely depend on the protein, the surface, and the solvent. This has to be taken into account when measuring the adsorbed amount of proteins with the QCM-D or deducing structural information such as layer thickness from optical measurements using an assumed refractive index.

Besides the consequences in the quantitative analysis of protein adsorption the possibility of measuring the density and refractive index of adsorbing protein layers also helps the understanding of the role of solvent in the adsorption process and provides information on the conformational changes of proteins (i.e., partial unfolding) upon contact with a surface.

REFERENCES

Arosio, D., E. Kwansa Herman, H. Gering, G. Piszczek, and E. Bucci. 2002. Static and dynamic light scattering approach to the hydration of hemoglobin and its supertetramers in the presence of osmolites. *Biopolymers.* 63:1–11.

Arwin, H. 2000. Ellipsometry on thin organic layers of biological interest: characterization and applications. Thin Solid Films. p 48–56.

Bailey, L. E., D. Kambhampati, K. K. Kanazawa, W. Knoll, and C. W. Frank. 2002. Using surface plasmon resonance and the quartz crystal microbalance to monitor in situ the interfacial behavior of thin organic films. *Langmuir.* 18:479–489.

Baird, C. L., and D. G. Myszka. 2001. Current and emerging commercial optical biosensors. *J. Mol. Recognit.* 14:261–268.

Ball, V., and J. J. Ramsden. 1998. Buffer dependence of refractive index increments of protein solutions. *Biopolymers.* 46:489–492.

Benesch, J., A. Askendal, and P. Tengvall. 2002. The determination of thickness and surface mass density of mesothick immunoprecipitate layers by null ellipsometry and protein (125)iodine labeling. *J. Colloid Interface Sci.* 249:84–90.

Cooper, M. A. 2002. Optical biosensors in drug discovery. *Nat. Rev. Drug Discov.* 1:515–528.

de Feijter, J. A., J. Benjamins, and F. A. Veer. 1978. Ellipsometry as a tool to study the ad-sorption of synthetic and biopolymers at the air-water interface. *Biopolymers.* 17:1759–1772.

Glasmastar, K., C. Larsson, F. Hook, and B. Kasemo. 2002. Protein adsorption on supported phospholipid bilayers. *J. Colloid Interface Sci.* 246:40–47.

Henderson, M. A. 2002. The interaction of water with solid surfaces: fundamental aspects revisited. *Surf. Sci. Rep.* 46:1–308.

Hook, F., B. Kasemo, T. Nylander, C. Fant, K. Sott, and H. Elwing. 2001. Variations in coupled water, viscoelastic properties, and film thickness of a Mefp-1 protein film during adsorption and cross- linking: A quartz crystal microbalance with dissipation monitoring, ellipsometry, and surface plasmon resonance study. *Anal. Chem.* 73:5796–5804.

Hook, F., J. Voros, M. Rodahl, R. Kurrat, P. Boni, J. J. Ramsden, M. Textor, N. D. Spencer, P. Tengvall, J. Gold, et al. 2002. A comparative study of protein adsorption on titanium oxide surfaces using in situ ellipsometry, optical waveguide lightmode spectroscopy, and quartz crystal microbalance/dissipation. *Colloid. Surface. B.* 24:155–170.

Horvath, R., J. Voros, R. Graf, G. Fricsovszky, M. Textor, L. R. Lindvold, N. D. Spencer, and E. Papp. 2001. Effect of patterns and inhomogeneities on the surface of waveguides used for optical waveguide lightmode spectroscopy applications. *Appl. Phys. B-Lasers O.* 72:1–7.

Jung, L. S., C. T. Campbell, T. M. Chinowsky, M. N. Mar, and S. S. Yee. 1998. Quantitative interpretation of the response of surface plasmon resonance sensors to adsorbed films. *Langmuir.* 14:5636–5648.

Kasemo, B. 2002. Biological surface science. *Surf. Sci.* 500:656–677.

Kull, T., T. Nylander, F. Tiberg, and M. Wahlgren. 1997. Effect of surface properties and added electrolyte on the structure of.beta.-casein layers adsorbed at the solid/aqueous interface. *Langmuir.* 13:5141–5147.

Kurrat, R., M. Textor, J. J. Ramsden, P. Boni, and N. D. Spencer. 1997. Instrumental improvements in optical waveguide light mode spectroscopy for the study of biomolecule adsorption. *Rev. Sci. Instrum.* 68: 2172–2176.

Laschitsch, A., B. Menges, and D. Johannsmann. 2000. Simultaneous determination of optical and acoustic thicknesses of protein layers using surface plasmon resonance spectroscopy and quartz crystal micro-weighing. *Appl. Phys. Lett.* 77:2252–2254.

Lu, J. R., T. J. Su, P. N. Thirtle, R. K. Thomas, A. R. Rennie, and R. Cubitt. 1998. The denaturation of lysozyme layers adsorbed at the hydrophobic solid/liquid surface studied by neutron reflection. *J. Colloid Interface Sci.* 206:212–223.

Lukosz, W. 1991. Principles and sensitivities of integrated optical and surface-plasmon sensors for direct affinity sensing and immunosensing. *Biosens. Bioelectron.* 6:215–225.

Malmsten, M. 2000. Protein adsorption at the solid-liquid interface. *In* Protein Architecture: Interfacing Molecular Assemblies and Immobilization Biotechnology. Y. Lvov and H. Möhwald, editors. Marcel Dekker, New York. 1–23.

Mann, E. K. 2001. Evaluating optical techniques for determining film structure: Optical invariants for anisotropic dielectric thin films. *Langmuir.* 17:5872–5881.

Mathieu, H. J. 2001. Bioengineered material surfaces for medical applications. *Surface Interface Anal.* 32:3–9.

Norde, W. 2000. Proteins at solid surfaces. *In* Physical Chemistry of Biological Interfaces. A. Baszkin and W. Norde, editors. Marcel Dekker, New York. 115–135.

O'Sullivan, C. K., and G. G. Guilbault. 1999. Commercial quartz crystal microbalances—theory and applications. *Biosens. Bioelectron.* 14:663–670.

Otzen, D. E., M. Oliveberg, and F. Hook. 2003. Adsorption of a small protein to a methyl-terminated hydrophobic surfaces: effect of protein-folding thermodynamics and kinetics. *Colloid. Surface. B.* 29:67–73.

Picart, C., G. Ladam, B. Senger, J. C. Voegel, P. Schaaf, F. J. G. Cuisinier, and C. Gergely. 2001. Determination of structural parameters characterizing thin films by optical methods: a comparison between scanning angle reflectometry and optical waveguide lightmode spectroscopy. *J. Chem. Phys.* 115:1086–1094.

Ramsden, J. J. 1993. Review of new experimental techniques for investigating random sequential adsorption. *J. Statistical Phys.* 73:853–877.

Ramsden, J. J. 1997. Optical biosensors. *J. Mol. Recognit.* 10:109–120.

Reimhult, E., F. Hook, and B. Kasemo. 2003. Intact vesicle adsorption and supported biomembrane formation from vesicles in solution: Influence of surface chemistry, vesicle size, temperature, and osmotic pressure. *Langmuir.* 19:1681–1691.

Rich, R. L., and D. G. Myszka. 2002. Survey of the year 2001 commercial optical biosensor literature. *J. Mol. Recognit.* 15:352–376.

Ruiz, L., E. Fine, J. Voros, S. A. Makohliso, D. Leonard, D. S. Johnston, M. Textor, and H. J. Mathieu. 1999. Phosphorylcholine-containing polyurethanes for the control of protein adsorption and cell attachment via photoimmobilized laminin oligopeptides. *J. Biomater. Sci. Polym. Ed.* 10:931–955.

Schaaf, P., P. Dejardin, A. Johner, and A. Schmitt. 1987a. Thermaldenaturation of an adsorbed fibrinogen layer studied by reflectometry. *Langmuir.* 3:1128–1131.

Schaaf, P., P. Dejardin, and A. Schmitt. 1987b. Reflectometry as a technique to study the adsorption of human-fibrinogen at the silica solution interface. *Langmuir.* 3:1131–1135.

Skladal, P., and J. Horacek. 1999. Kinetic studies of affinity interactions: comparison of piezoelectric and resonant mirror-based biosensors. *Anal. Lett.* 32:1519–1529.

Stalgren, J. J. R., J. Eriksson, and K. Boschkova. 2002. A comparative study of surfactant adsorption on model surfaces using the quartz crystal microbalance and the ellipsometer. *J. Colloid Interface Sci.* 253:190–195.

Talbot, J., G. Tarjus, P. R. Van Tassel, and P. Viot. 2000. From car parking to protein adsorption: an overview of sequential adsorption processes. *Colloid. Surf. A.* 165:287–324.

Tiefenthaler, K., and W. Lukosz. 1989. Sensitivity of grating couplers as integrated-optical chemical sensors. *J. Opt. Soc. Am. B.* 6:209–220.

Tsai, C.-J., J. V. Maizel, Jr., and R. Nussinov. 2002. The hydrophobic effect: a new insight from cold denaturation and a two-state water structure. *Crit. Rev. Biochem. Mol. Biol.* 37:55–69.

Tsai, J., R. Taylor, C. Chothia, and M. Gerstein. 1999. The packing density in proteins: standard radii and volumes. *J Mol Biol.* 290:253–266.

Vikinge T. P., K. M. Hansson, P. Sandstrom, B. Liedberg, T. L. Lindahl, I. Lundstrom, P. Tengvall, and F. Hook. 2000. Comparison of surface plasmon resonance and quartz crystal microbalance in the study of whole blood and plasma coagulation. *Biosensors Bioelectronics.* 15:605–613.

Vogler, E. A. 1998. Structure and reactivity of water at biomaterial surfaces. *Adv. Colloid Interface Sci.* 74:69–117.

Voinova, M. V., M. Jonson, and B. Kasemo. 2002. 'Missing mass' effect in biosensor's QCM applications. *Biosensors Bioelectron.* 17:835–841.

Voros, J., J. J. Ramsden, G. Csucs, I. Szendro, S. M. De Paul, M. Textor, and N. D. Spencer. 2002. Optical grating coupler biosensors. *Biomaterials.* 23:3699–3710.

Welsch, W., C. Klein, M. vonSchickfus, and S. Hunklinger. 1996. Development of a surface acoustic wave immunosensor. *Anal. Chem.* 68:2000–2004.

Widmer, M. R., M. Heuberger, J. Voros, and N. D. Spencer. 2001. Influence of polymer surface chemistry on frictional properties under protein-lubrication conditions: implications for hip-implant design. *Tribol. Lett.* 10:111–116.

Yoldas, B. E. 1982. Deposition and properties of optical oxide coatings from polymerized solutions. *Appl. Opt.* 21:2960–2964.